[Article] www.whxb.pku.edu.cn

HCOO 在 Cu(110)、Ag(110)和 Au(110)表面的吸附

庞先勇[1] 邢 斌[1] 王贵昌[2,*] YOSHITADA Morikawa[3]
JUNJI Nakamura[4]
([1] 太原理工大学化学化工学院, 太原 030024; [2] 南开大学化学学院理论与计算化学中心, 天津 300071;
[3] Institute of Scientific and Industrial Research (ISIR), Osaka University, 8-1 Mihogaoka, Osaka 567-0047, Japan;
[4] Institute of Materials Science, University of Tsukuba, Tennoudai 1-1-1, Tsukuba, Ibaraki 305-8573, Japan)

摘要: 采用密度泛函理论(DFT)以及广义梯度近似方法(GGA)计算了甲酸根(HCOO)在 Cu(110)、Ag(110)和 Au(110)表面的吸附. 计算结果表明, 短桥位是最稳定的吸附位置, 计算的几何参数与以前的实验和计算结果吻合. 吸附热顺序为 Cu(110)(−116 kJ·mol^{-1})>Ag(110)(−57 kJ·mol^{-1})>Au(110)(−27 kJ·mol^{-1}), 与实验上甲酸根的分解温度相一致. 电子态密度分析表明, 吸附热顺序可以用吸附分子与金属 *d*-带之间的 Pauli 排斥来关联, 即排斥作用越大, 吸附越弱. 另外还从计算的吸附热数据以及实验上 HCOO 的分解温度估算了反应 CO_2+1/2H_2→HCOO 的活化能, 其大小顺序为 Au(110)>Ag(110)>Cu(110).

关键词: 化学吸附; 甲酸根; Cu(110); Ag(110); Au(110); DFT-GGA-slab
中图分类号: O641; O647

Formate Adsorption on Cu(110), Ag(110) and Au(110) Surfaces

PANG Xian-Yong[1] XING Bin[1] WANG Gui-Chang[2,*] YOSHITADA Morikawa[3] JUNJI Nakamura[4]
([1]*College of Chemistry and Chemical Engineering, Taiyuan University of Technology, Taiyuan 030024, P. R. China*;
[2]*Center of Theoretical Computational Chemistry, College of Chemistry, Nankai University, Tianjin 300071, P. R. China*;
[3]*Institute of Scientific and Industrial Research (ISIR), Osaka University, 8-1 Mihogaoka, Osaka 567-0047, Japan*;
[4]*Institute of Materials Science, University of Tsukuba, Tennoudai 1-1-1, Tsukuba, Ibaraki 305-8573, Japan*)

Abstract: The adsorption of formate (HCOO) on Cu(110), Ag(110), and Au(110) surfaces has been studied by the density functional theory (DFT) and generalized gradient approximation (GGA) with slab model. To find the most stable adsorption site of HCOO on M(110) (M=Cu, Ag, Au), we investigated several adsorption forms like bidentate and monodentate adsorption sites. The calculated results show that the most stable adsorption site is short-bridge bidentate form for all the three metals, which is independence of the metallic lattice constants. The calculated atomic geometries agree well with the experimental results and the previous calculation results. Adsorption energy of formate follows the order of Cu(110) (−116 kJ·mol^{-1})>Ag(110)(−57 kJ·mol^{-1})>Au(110)(−27 kJ·mol^{-1}), in agreement with decomposition temperature of formate measured by experiments. The order of the adsorption energy can be explained by Pauli repulsion between molecular orbitals of formate with *d*-band of metal, i.e., the more occupied population of formate, the larger Pauli repulsion, which results in the weaker adsorption of formate. In addition, the activation energy of formate synthesis from CO_2 and H_2 was predicated using the adsorption energy of formate and the decomposition temperature of formate, which follows the order of Au(110)>Ag(110)>Cu(110).

Key Words: Chemisorption; Formate; Cu(110); Ag(110); Au(110); DFT-GGA-slab

Received: February 19, 2009; Revised: March 18, 2009; Published on Web: April 24, 2009.

*Corresponding author. Email: wangguichang@nankai.edu.cn; Tel: +86-22-23503824.

The project was supported by the National Natural Science Foundation of China (20273034, 20673063) and Found for the Star of Nankai, China.
国家自然科学基金(20273034, 20673063)和"南开之星"资助

© Editorial office of Acta Physico-Chimica Sinica

Formate, HCOO, is an important intermediate species in the methanol synthesis and the water-gas shift reaction over transition metals, and has been investigated by many researchers both in experiment and calculation[1-7]. The experimental studies on the surface structures of formate using the technologies, such as surface extended X-ray absorption fine structure (SEXAFS)[1], near-edge X-ray absorption fine structure (NEXAFS)[2] and photoelectron diffraction (PhD)[3], have shown that formate oriented with its molecular plane normal to the metal surfaces and short-bridge bidentate formate was the most stable form on both Cu(110) and Cu(100) surfaces. The oxygen atoms of formate were located at the same distance from the surface with the nearest neighboring Cu—O distance of (0.198±0.004) nm[3]. On the Ag(110) surface, NEXAFS results[4] suggest that chelating-bridge site (see Fig.1) was the preferred adsorption site. On the other hand, theoretical calculations using cluster model[6,7] have shown that bidentate formate on the short-bridge site was most stable on both Cu(110) and Ag(110) surfaces. As for kinetic experiments, Outka *et al.*[5] have reported that the decomposition temperature of formate followed the order of Cu>Ag>Au.

It is well known that the slab model is considered to be more suitable for the extended system such as solid and surface states, while the cluster model is generally suitable for the isolated molecules in gas phase[8-10]. In addition, the slab model can treat the interactions between adsorbates, which are ignored in the cluster model calculation. In the present study, we carried out DFT-GGA calculation with slab model to study HCOO adsorption on Cu(110), Ag(110) and Au(110) surfaces to answer the following questions: (1) Which adsorption form is preferred for the adsorption of HCOO (short-bridge or chelating-bridge site) and how different is the adsorption energy on these three metals? (2) What is the factor determining the order in the adsorption energy of HCOO for these three metals? (3) Is there a clear relationship between HCOO adsorption energy and its decomposition temperature?

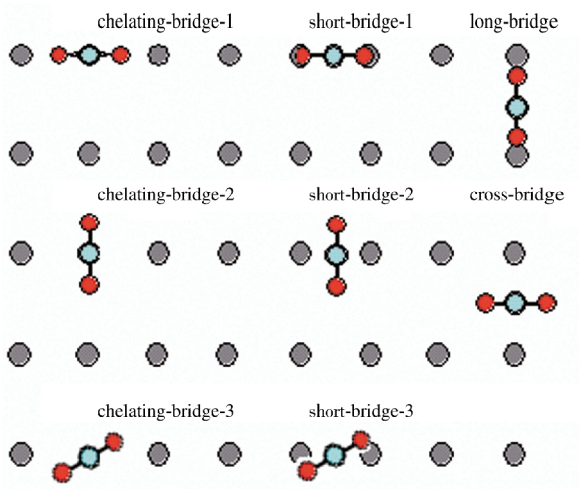

Fig.1 Possible adsorption sites of HCOO on the M(110) (M=Cu, Ag, Au) surface with the bidentate form

1 Calculation method and models

All calculations based on a generalized gradient approximation in the density functional theory were carried out using a package "STATE" (simulation tool for atom technology) which has been successfully applied to adsorption problems in the case of semiconductor and metal surfaces[11-14]. GGA with Perdew, Burke, and Ernzerhof functional is used for the exchange and correlation energy calculation[15]. Ionic cores are described by Vanderbilt's ultrasoft pseudopotentials[16] and valence electrons are expanded with a plane wave basis set. The energy cutoffs of the plane wave basis sets are 32834 and 525346 kJ·mol^{-1} for wave functions and charge density, respectively. In order to model the HCOO coverage, the unit cell of $p(3\times2)$ with three and six layers are used, and a vacuum region of 1 nm was used in between two neighboring slabs. The surface Brillouin zone is sampled using a 4×4×1 special k-point for M(110) (M=Cu, Ag, Au) surface. For the structure optimization, the adsorbed HCOO species and one top layer (for three-layer model), and three-layer (for six-layer model) of substrate atoms are allowed relaxed until the maximum force on the atom is smaller than 496 kJ·mol^{-1}·nm^{-1}. Before the calculation, we first calculate the metallic lattice constants to test the correction of the Vanderbilt's ultrasoft pseudopotentials used in this work. The DFT lattice constants of Cu, Ag and Au are 0.3644, 0.4069, and 0.4135 nm, respectively, which are generally agreement with the experimental data[17]. Then, the bond energy of O_2 calculation is used to examine the energy cutoffs for oxygen. The calculated bond energies of O_2 are 431, 432 and 432 kJ·mol^{-1} for the energy cutoff of 32834, 39729 and 47281 kJ·mol^{-1}, respectively. Since the bond energy is almost the same for the different energy cutoff, which means the chosen oxygen energy cutoff is reasonable.

2 Results and discussion

There are a few possible adsorption sites for the adsorption of formate on the M(110) (M=Cu, Ag, Au) surfaces. The most stable adsorption site was first determined using a three-layer slab model with one layer relaxed. After that, the adsorption energies for the most stable site were calculated using a six-layer slab model with three layers relaxed. The adsorption energy (Q) was defined with respect to the potential energy of gaseous CO_2 and H_2 and was calculated by the following formula:

$$Q=E_{M\_HCOO}-E_M-E_{CO_2}-1/2E_{H_2}$$

where E is the calculated total energy for corresponding species. In fact, Q is equal to the heat of reaction (ΔH) for the formate synthesis from gaseous CO_2 and $1/2H_2$. Here, negative value of Q means strong adsorption.

2.1 HCOO/Cu(110)

The calculated adsorption energies, optimized equilibrium structures of HCOO adsorbed on different sites of Cu(110) as well as experimentally determined structures of HCOO are listed in Table 1. Formate has two kinds of adsorption forms: one is bidentate HCOO with two oxygen atoms bound to the Cu surface, and another adsorption form is monodentate HCOO with

Table 1 DFT-GGA results of adsorption energies (Q), and optimized geometries for HCOO adsorbed on the different sites of M(110) (M=Cu, Ag, Au) surfaces

Metal	Model	Adsorption site	Structure				Q/(kJ·mol^{-1})
			R(C—H)/nm	R(C—O)/nm	R(O—M)/nm	A(OCO)/(°)	
Cu(110)	3-layer	short-bridge-1	0.111	0.127	0.197	127.50	−97
		short-bridge-2	0.111	0.127	0.246	123.67	8
		short-bridge-3	–	–	–	–	move to short-bridge-1
		long-bridge	0.111	0.127	0.179	126.50	−82
		cross-bridge	0.111	0.127	0.163	127.10	24
		chelating-bridge-1	0.111	0.128	0.226	124.81	−41
		chelating-bridge-2	0.111	0.127	0.216	122.92	−5
		chelating-bridge-3	0.111	0.127	0.225	123.35	−10
		mono-dentate	0.111	0.127	0.201	126.32	−18
	6-layer	short-bridge-1	0.111	0.127	0.197	127.50	−116
		mono-dentate	0.111	0.127	0.202	126.31	−31
Ag(110)	3-layer	short-bridge-1	0.111	0.127	0.216	129.33	−44
		short-bridge-2	0.111	0.127	0.266	125.02	12
		short-bridge-3	–	–	–	–	move to short-bridge-1
		long-bridge	0.111	0.127	0.219	131.74	−31
		cross-bridge	0.111	0.127	0.293	128.10	50
		chelating-bridge-1	0.111	0.128	0.241	125.10	−10
		chelating-bridge-2	0.111	0.128	0.240	125.55	8
		chelating-bridge-3	0.110	0.127	0.242	125.52	0
		mono-dentate	0.111	0.134	0.229	127.00	21
	6-layer	short-bridge-1	0.111	0.127	0.216	129.32	−57
		mono-dentate	0.111	0.127	0.219	131.54	−6
Au(110)	3-layer	short-bridge-1	0.111	0.127	0.221	130.42	−14
		short-bridge-2	0.111	0.127	0.271	126.50	52
		short-bridge-3	–	–	–	–	move to short-bridge-1
		long-bridge	0.111	0.127	0.220	132.31	11
		cross-bridge	0.111	0.127	0.300	128.32	91
		chelating-bridge-1	0.111	0.127	0.246	126.31	15
		chelating-bridge-2	0.111	0.127	0.246	125.06	40
		chelating-bridge-3	0.110	0.127	0.242	125.00	47
		mono-dentate	0.111	0.134	0.233	127.80	50
	6-layer	short-bridge-1	0.111	0.127	0.221	130.40	−27
		mono-dentate	0.111	0.134	0.233	127.64	40

R(O—M) is the distance between oxygen atom and the nearest-neighbor metal atom.

only one oxygen bound to the Cu surface. For the former one, there are several possible adsorption sites as shown in Fig.1, including short-bridge, long-bridge, chelating-bridge and cross-bridge sites. In Table 1, one can see that the short-bridge site is the most stable adsorption site due to its largest negative in the adsorption energy (−97 kJ·mol^{-1}) among the different sites, the second stable site is long-bridge, and the cross-bridge site is the most unstable one with the smallest adsorption energy (even a positive data: 24 kJ·mol^{-1}). The calculated results agree with experimental results that bidentate HCOO on short-bridge site is observed[1−3,6]. In addition, monodentate HCOO observed by the FTRAIRS (Fourier-transform reflection/absorption IR spectroscopy) experiments at 200 K converts into bidentate HCOO at a higher temperature (300 K)[18]. Although the adsorption energy of monodentate HCOO is as small as 18 kJ·mol^{-1}, it is possible to exist on the Cu surface at low temperatures or as an intermediate of catalytic reactions such as decomposition of formic acid.

For the stable short-bridge HCOO, the optimized C—O bond length is 0.127 nm, the O—C—O angle is 127.50°, and the distance between the oxygen atom and the nearest neighboring copper atom is 0.197 nm, which is in agreement with the experimental data of (0.198±0.004) nm[1−3] and the previous calculated results[6,19].

In order to obtain more accurate adsorption energy for the most stable short-bridge site, four, five, and six-layer slab models were used, and the corresponding data are −115, −100, and −116 kJ·mol^{-1}, respectively. However, the difference between three-layer and six-layer models is not so significant. This is contrast to the cluster model calculation, in which the adsorption energies are very sensitive to the cluster size[19]. Moreover, our calculation results for the adsorption energy of short-bridge HCOO, −97 and −116 kJ·mol^{-1} for three-layer and six-layer models, respectively, are much more close to kinetic experimental data (−85 kJ·mol^{-1} [20]) than the previous cluster calculation result (−171 kJ·mol^{-1} [19]).

2.2 HCOO/Ag(110)

The calculated adsorption energies as well as the equilibrium structures for HCOO on the various sites of Ag(110) are listed in Table 1. For the possible adsorption sites, the short-bridge HCOO shows the largest negative in the adsorption energy (−44 kJ·mol^{-1}),

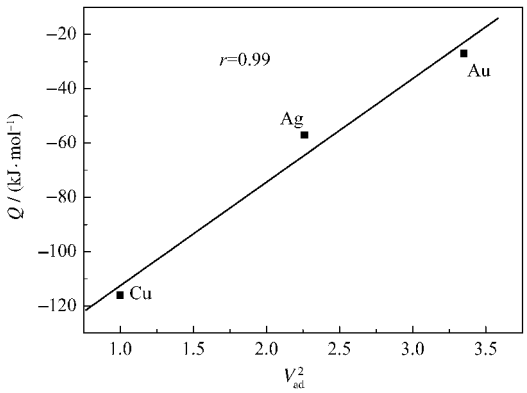

Fig.2 Plot of HCOO adsorption energy (Q) *versus* coupling matrix element squared (V_{ad}^2) for six-layer slab model

suggesting that the short-bridge site is the most stable form on Ag(110). On the other hand, mono-dentate HCOO shows a positive value, indicating that mono-dentate HCOO is difficult to be formed, which is contrast to the case of Cu(110). For the short-bridge HCOO and monodentate HCOO, additional calculations using the six-layer slab model with three layers relaxed give the values of −57 and −6 kJ·mol^{-1}, respectively. The calculated results here for the structure of the short-bridge adsorption site are in good agreement with the previous calculation result based on the cluster model (R(C—O)=0.125 nm, R(C—H)=0.112 nm, R(O—Cu)=0.221 nm, and A(OCO)=129.80° [7]).

2.3 HCOO/Au(110)

Calculated adsorption energies of HCOO at various sites on Au(110) are listed in Table 1 with the optimized structures of HCOO. Like Cu(110) and Ag(110) surfaces, short-bridge HCOO is the most stable site (with the largest negative adsorption energy of −14 kJ·mol^{-1} (−27 kJ·mol^{-1} for six-layer model)). This is, however, much larger than those of Cu(110) and Ag(110).

Based on the above calculation results, we know that the perfected adsorption site of HCOO on the M(110) (M=Cu, Ag, Au) surfaces is the same, i.e., bi-dentate short-bridge site even though the increasing of the nearest neighbor metal-metal(M—M) distance from Cu(0.256 nm) to Ag(or Au) (0.289 nm).

2.4 Difference in adsorption energy among three metals

Table 1 shows that the adsorption energy of HCOO with the order of Cu(110)>Ag(110)>Au(110). This trend can be explained by Pauli repulsion. It is well known that Pauli repulsion significantly contributes to the adsorption system for *d*-closed metals like Cu, Ag and Au[21]. It has been regarded as the main factor controlling the variation in adsorption energy from Cu to Au. In general, the stronger of the overlap, the larger of the repulsion, and the weaker of adsorption energy. To see the effect of Pauli repulsion, we first use the coupling matrix element squared (V_{ad}^2)[21] to correlate HCOO adsorption energy (Fig.2) (V_{ad}^2 is a quantity to measure the interaction between adsorbate and metallic *d*-band). From the fitted line in Fig.2, the adsorption energy, Q, is expressed as an equation, $Q=-151+38V_{ad}^2$, where the contribution of *sp* electrons to attractive force is by far large (the constant is −151) and that the contribution from *d* electrons is purely repulsion. This conclusion agrees with the previous conclusion based on the slab model[13,14] as well as the cluster model[22] calculations that the metallic *sp* electron is the dominant factor to the binding energy, while the *d* electron is the change trend for the different metals. It should be pointed out that the V_{ad}^2 comes from the overlap population between atomic N and IB metallic *d*-band[21]. To gain more insight into the adsorption nature of HCOO, the overlap population integral (S_{ij}^2) of the HCOO molecular orbital with the metals is also calculated based on the projected density of state (PDOS) onto HCOO molecular orbital (Fig.3). It is indicated that the HCOO/Au(110) adsorption system shows the largest total overlap (6.81), while the HCOO/Cu(110) adsorption system shows the smallest overlap (4.75). That is, the order of overlap population among surfaces of these three metals is the same as that of the HCOO adsorption energy, which is also agreement with the above discussion based on the V_{ad}^2.

2.5 Comparison to kinetic experiments

As for Cu(110), the adsorption energy of bidentate HCOO can be experimentally estimated to be −85 kJ·mol^{-1} by the difference in activation energy between forward and backward formate synthesis[20]. This value is in good agreement with those calculated on Cu(110) in the present study, i.e., −97 and −116 kJ·mol^{-1} for three-layer and six-layer models, respectively. On Au(110) and Ag(110), the synthesis of HCOO from CO_2 and H_2 has not been carried out so that the experimental adsorption energies of HCOO are unknown. However, it has been reported that HCOO is decomposed into CO_2 and 1/2H_2 on Au(110), Ag(110), and Cu(110) with peak maximum at 340, 408, and 475 K, respectively, in the temperature-programmed reaction experiments[23].

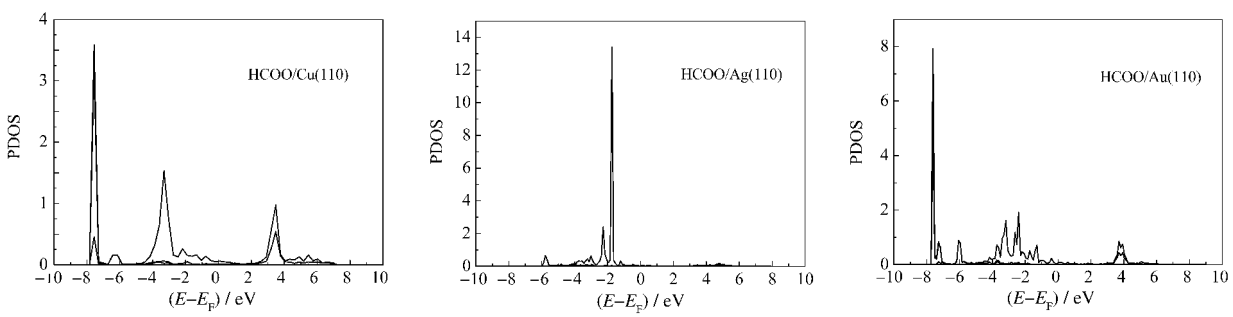

Fig.3 Projected density of state (PDOS) onto HCOO molecular orbital

E_F is the energy of Fermi level.

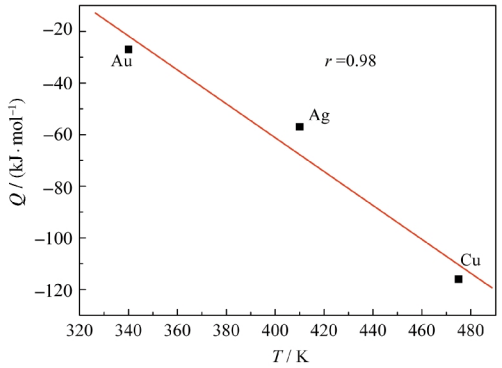

Fig.4 Correlation between HCOO adsorption energy and its decomposition temperature

That is, the energy barrier for the decomposition of HCOO follows the order of Au(110)<Ag(110)<Cu(110)[5,24]. This is consistent with the order of Au(110)<Ag(110)<Cu(110) in the adsorption energy of HCOO as shown in Table 1. The correlation between the calculated adsorption energy and decomposition temperature was thus examined as shown in Fig.4. It reveals that the adsorption energy is proportional to the decomposition temperature, corresponding to the decomposition barrier (known as the so called Brönsted-Evans-Polanyi principle[23,25]). This suggests that the present calculation is valid, although the adsorption energy has not been determined experimentally for Au(110) and Ag(110). Our previous isothermal experiments have shown that the activation energy of formate decomposition is 145 kJ·mol^{-1} on Cu(110)[20]. Assuming that the decomposition peak temperature of HCOO described above, is proportional to the activation energy of HCOO decomposition, the activation energies of HCOO decomposition on Au(110) and Ag(110) were evaluated to be 104 and 124 kJ·mol^{-1}, respectively, using the Cu(110) data. Based on the calculated adsorption energy and the estimated decomposition barrier, the energy barrier for the HCOO formation from CO_2 and 1/2 H_2, E_a', can be predicted by using the formula of $E_a'=E_a+\Delta H$, where E_a is the activation energy of HCOO decomposition, ΔH is the heat of reaction. Since the ΔH is equal to the HCOO adsorption energy in this work, and thus the predicated HCOO formation barriers are 77 and 67 kJ·mol^{-1} on Au(110) and Ag(110), respectively. The formation barriers of HCOO formation on Au(110) and Ag(110) are greater compared to the Cu(110) case, i.e., 60 and 62 kJ·mol^{-1} obtained in experiment and calculation, respectively[20]. The kinetic measurement of HCOO synthesis on Cu surface is possible only for high pressure measurements, meaning that the reaction rate is so small. It is thus expected that the HCOO synthesis is much more slow on Au(110) and Ag(110).

3 Conclusions

A DFT-GGA slab model has been used to study the adsorption of formate on Cu(110), Ag(110) and Au(110) surfaces. The calculated results show that the most stable adsorption site is the short-bridge bidentate for all the three metals although the nearest distance between metals increases from Cu to Ag (or Au). In the meantime, the equilibrium structures for the adsorbed formate are in agreement with the experimental results as well as the previous calculation results. Furthermore, the calculated adsorption energies of HCOO are −116, −57, and −27 kJ·mol^{-1} on Cu(110), Ag(110) and Au(110), respectively. These data can be used to explain the chemical activity of HCOO decomposition on Cu(110), Ag(110), and Au(110), i.e., the stronger adsorption of HCOO, the more difficult to decompose to CO_2 and H_2.

References

1 Crapper, M. D.; Riley, C. E.; Woodruff, D. P.; Puschmann, A.; Haase, J. *Surf. Sci*., **1986, 171**: 1

2 Somers, J.; Robinson, A. W.; Lindner, T.; Ricken, D.; Bradshaw, A. M. *Phys. Rev. B*, **1989, 40**: 2053

3 Woodruff, D. P.; McConville, C. F.; Kilcoyne, A. L. D.; Lindner, T.; Somers, J.; Surman, M.; Paolucci, G.; Bradshaw, A. M. *Surf. Sci*., **1988, 201**: 228

4 Stevens, P. A.; Madix, R. J.; Stohr, J. *Surf. Sci*., **1990, 230**: 1

5 Outka, D. A.; Madix, R. J. *Surf. Sci*., **1987, 179**: 361

6 Gomes, J. R. B.; Gomes, J. A. N. F. *Surf. Sci*., **1999, 432**: 279

7 Maurizio, C.; Chiara, M.; Andrea, V. *J. Chem. Soc. Faraday Transactions*, **1998, 94**: 797

8 Michaelides, A.; Hu, P. *J. Am. Chem. Soc*., **2000, 122**: 9866

9 Greeley, J.; Mavrikakis, M. *J. Am. Chem. Soc*., **2002, 124**: 7193

10 Mortensen, J. J.; Hansen, L. B.; Hammer, B.; Nørskov, J. K. *J. Catal*., **1999, 182**: 479

11 Morikawa, Y.; Iwata, K.; Nakamura, J.; Fujitani, T.; Terakura, K. *Chem. Phys. Lett*., **1999, 304**: 91

12 Wang, G. C.; Zhou, Y. H.; Morikawa, Y.; Nakamura, J.; Cat, Z. S.; Zhao, X. Z. *J. Phys. Chem., B*, **2005, 109**: 12431

13 Wang, G. C.; Zhou, Y. H.; Nakamura, J. *J. Chem. Phys*., **2005, 122**: 044707

14 Wang, G. C.; Li, J.; Xu, X. F.; Li, R. F.; Nakamura, J. *J. Comput. Chem*., **2005, 26**: 871

15 Perdew, J. P.; Burke, K.; Ernzerhof, M. *Phys. Rev. Lett*., **1996, 77**: 3865

16 Vanderbilt, D. *Phys. Rev. B*, **1990, 41**: 7892

17 Lide, D. R. CRC handbook of chemistry and physics. 73rd ed. Boca Raton: CRC Press, 1992−1993

18 Bowker, M.; Haq, S.; Holroyd, R.; Parlett, P. M.; Poulston, S.; Richardson, N. *J. Chem. Soc. Faraday Transactions*, **1996, 92**: 4683

19 Hu, Z. M.; Boyd, R. J. *J. Chem. Phys*., **2000, 112**: 9562

20 Nakamura, I.; Nakano, H.; Fujitani, T.; Uchijima, T.; Nakamura, J. *J. Vac. Sci. Technol. A*, **1999, 17**: 1592

21 Hammer, B.; Nørskov, J. K. *Adv. Catal*., **2000, 45**: 71

22 Whitten, J. L.; Yang, H. *Surf. Sci. Rep*., **1996, 24**: 55

23 Evans, M. G.; Polanyi, M. *Trans. Faraday. Soc*., **1936, 32**: 1333

24 Mavrikakis, M.; Barteau, M. A. *J. Mol. Catal. A-Chem*., **1998, 131**: 135

25 Sheth, P. A.; Neurock, M.; Smith, C. M. *J. Phys. Chem. B*, **2005, 109**: 12449